Radiative Heat Transfer with a Cylindrical Waveguide Decays Logarithmically Slow

Kiryl Asheichyk[1,*] and Matthias Krüger[2,†]
[1]Department of Theoretical Physics and Astrophysics, Belarusian State University, 5 Babruiskaya Street, 220006 Minsk, Belarus
[2]Institute for Theoretical Physics, Georg-August-Universität Göttingen, 37073 Göttingen, Germany

(Received 18 May 2022; accepted 28 September 2022; published 21 October 2022)

Radiative heat transfer between two far-field-separated nanoparticles placed close to a perfectly conducting nanowire decays logarithmically slow with the interparticle distance. This makes a cylinder an excellent waveguide which can transfer thermal electromagnetic energy to arbitrary large distances with almost no loss. It leads to a dramatic increase of the heat transfer, so that, for almost any (large) separation, the transferred energy can be as large as for isolated particles separated by a few hundred nanometers. A phenomenologically found analytical formula accurately describes the numerical results over a wide range of parameters.

DOI: 10.1103/PhysRevLett.129.170605

Heat radiation (HR) and radiative heat transfer (HT) are very sensitive to changes in geometrical configuration and material properties when the system length scales are smaller or comparable to the thermal wavelength (roughly 8 μm at room temperature). This was first observed more than 50 years ago for the HT between two parallel plates, where the near-field HT shows a strong increase with decreasing the gap width due to the evanescent waves contribution, absent for far-field separations [1,2]. Since then, researchers investigated near-field HR and HT in a variety of systems with objects of different shapes and materials, revealing plenty of interesting effects [3–6].

An important question is whether these near-field effects can be propagated to the far field, thereby improving the efficiency of HT between objects at large separations. Recent studies found such a propagation possible in two cases: (i) for anisotropic objects with some of their dimensions smaller than the thermal wavelength [7–9]; (ii) for objects that are placed in the proximity of intermediate objects [10–18]. In the first case, the far-field HT can greatly exceed the blackbody result, and for distances larger than the objects themselves, it decreases with the expected power law behavior [7–9].

The second case also provides a variety of interesting phenomena. The HT between two nanoparticles placed above a plate [10,13–16,18], inside a two-plates cavity [10,15], or connected through the near field by a sphere [12] can be enhanced by several orders of magnitude (compared to isolated particles) even for interparticle distances larger than the thermal wavelength. This enhancement and its mechanism strongly depend on the system geometry and material properties. A larger increase of the HT is achieved when the system supports resonant surface modes, for example, two SiC particles above a SiC plate [10,13–16,18] or inside a SiC cavity [15]. However, as the interparticle distance grows, the effect is quickly diminished due to a strong absorption of the SiC plates [10,13–15]. Less absorbing metallic plates provide a longer ranged, but smaller effect [13,15]. Using sophisticated structures can improve the efficiency, however, only in a short range of far-field separations [16–18]. Is there a geometry that allows for a long range energy transport beyond the mentioned scales?

In this Letter, we show that the HT between two far-field-separated nanoparticles placed in the proximity of a perfectly conducting cylinder is much larger than in other configurations studied before. It decays logarithmically as a function of the interparticle distance d, compared to d^{-2} decay for the particles in vacuum [19] or d^{-1} for the particles placed in a metallic cavity [15]. As a consequence of the logarithmic decay, the ratio to the HT for isolated particles grows as d^2, e.g., exceeding it by 12 orders of magnitude with d in the range of centimeters. Saying it differently, the HT at almost any large distance is comparable to the transfer between isolated particles at $d \approx 500$ nm for the parameters studied. We analyze the dependence of the HT on the system parameters, providing a phenomenological analytical formula, and discuss potential applications and implications of the observed phenomena.

The considered system is depicted in Fig. 1. Two spherical particles are placed symmetrically in the proximity of an infinitely long perfectly conducting cylinder. We aim to compute the HT from particle 1 at temperature T_1 to particle 2. In general, there are other HT contributions, due to sources in the environment, the cylinder (if not a perfect conductor), and particle 2 [20]. The studied contribution depends only on T_1, and may be imagined, e.g., as the case with all temperatures except for T_1 equal to zero.

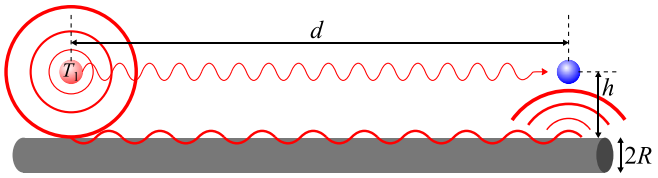

FIG. 1. Radiative heat transfer from particle 1 at temperature T_1 to particle 2 in the presence of an infinitely long perfectly conducting cylinder of radius R. The near-field energy radiated by the first particle is captured by the cylinder and guided via surface waves to the second particle. These surface waves decay logarithmically slow with d, resulting in a highly efficient heat transfer even for far-separated particles.

Aiming at a proof of concept, and to simplify the problem, we use the point particle (PP) limit, where the two particles are small compared to the thermal wavelength, the particle's skin depth, and distances d and h [12,15,21]. The results in Figs. 2, 3, and 4 are valid for particle radii $R_i \ll h$, i.e., $R_i \approx 10$ nm or smaller for the given value of $h = 100$ nm.

Problems of HR and HT in many-body systems can be studied within frameworks of fluctuational electrodynamics [22,23] and scattering theory [24–26]. For our system, the HT from PP 1 to PP 2 reads as [12,24]

$$H = \frac{32\pi\hbar}{c^4}\int_0^\infty d\omega \frac{\omega^5}{e^{\frac{\hbar\omega}{k_B T_1}}-1}\mathrm{Im}(\alpha_1)\mathrm{Im}(\alpha_2)\mathrm{Tr}(\mathbb{G}\mathbb{G}^\dagger), \quad (1)$$

where c is the speed of light in vacuum, and $\hbar$ and k_B are Planck's and Boltzmann's constants, respectively. $\mathrm{Tr}(\mathbb{G}\mathbb{G}^\dagger)$ is the trace of the matrix product of the dyadic Green's function (GF) $\mathbb{G}$ of the cylinder, evaluated at the particles' coordinates, and its conjugate transpose $\mathbb{G}^\dagger$. The GF encodes the system geometry (it is a function of R, h, and d), and hence determines the role of the cylinder in the HT. Note that it is also a function of the wave number $k = \omega/c$ (i.e., the absolute value of the wave vector) or the corresponding wavelength $\lambda = 2\pi/k$.

$$\alpha_i(\omega) = \frac{\varepsilon_i(\omega)-1}{\varepsilon_i(\omega)+2}R_i^3 \quad (2)$$

is the electrical dipole polarizability of particle i, with R_i and ε_i being the radius and the frequency-dependent dielectric permittivity, respectively. Polarizabilities determine the radiation and absorption strength of the particles. For numerical illustration, we use both particles to be made of SiC, $\varepsilon_1 = \varepsilon_2 = \varepsilon_{\mathrm{SiC}}$, where [27]

$$\varepsilon_{\mathrm{SiC}}(\omega) = \varepsilon_\infty \frac{\omega^2-\omega_{\mathrm{LO}}^2+i\omega\gamma}{\omega^2-\omega_{\mathrm{TO}}^2+i\omega\gamma}, \quad (3)$$

with $\varepsilon_\infty = 6.7$, $\omega_{\mathrm{LO}} = 1.82\times10^{14}\,\mathrm{rad\,s^{-1}}$, $\omega_{\mathrm{TO}} = 1.48\times10^{14}\,\mathrm{rad\,s^{-1}}$, and $\gamma = 8.93\times10^{11}\,\mathrm{rad\,s^{-1}}$.

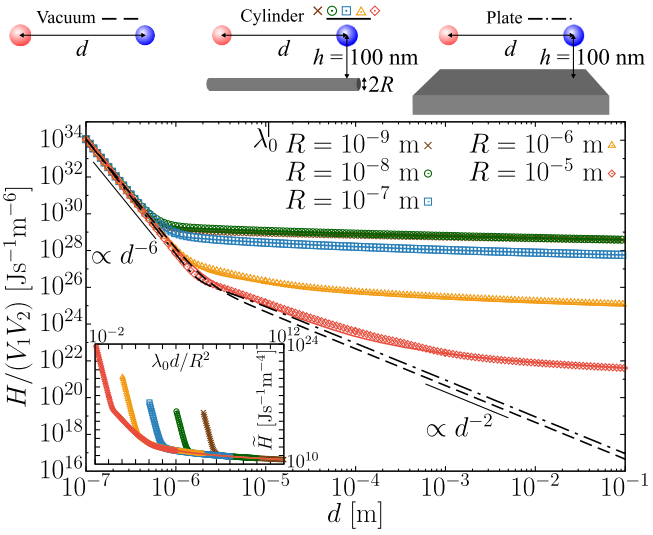

FIG. 2. Heat transfer (normalized by particles' volumes) from SiC particle 1 at temperature $T_1 = 300$ K to SiC particle 2 in the presence of a perfectly conducting cylinder as a function of interparticle distance d. The particles are placed symmetrically above the cylinder at distance $h = 10^{-7}$ m from its surface (see the sketch). The results are given for different radii R of the cylinder and compared to cases of the particles in vacuum and above a perfectly conducting plate at the same h. Points show numerically exact results [computed using Eq. (1), with numerically exact $\mathrm{Tr}(\mathbb{G}\mathbb{G}^\dagger)$], while solid lines represent the approximate HT given by formula (6). The dominant wavelength $\lambda_0 \approx 1.08\times10^{-5}$ m. Inset shows rescaled curves, $\widetilde{H} = H(R+h)^4/(V_1V_2\lambda_0^2)$ (same color coding), as a function of the rescaled distance $\lambda_0 d/R^2$ [see main text below Eq. (6)].

For details of the GF, we refer the reader to Supplemental Material [28]. It is worth noticing that the GF of a cylinder contains both integration over a certain component of the wave vector and summation over multipoles [28,29], in contrast to the GF of a plate (only integration) [12–14,16–18,30] or a sphere (only summation) [12]. This makes the numerical computations difficult requiring long computation times.

As for the system parameters, we fix $T_1 = 300$ K, such that the corresponding thermal and dominant wavelengths are $\lambda_{T_1} \approx 7.63\times10^{-6}$ m and $\lambda_0 \approx 1.08\times10^{-5}$ m, respectively, the latter resulting from the material properties of Eq. (3) and the polarizability in Eq. (2). The particles are placed at a small near-field distance above the cylinder, $h = 10^{-7}$ m, for a strong coupling between particles and cylinder. The dependence on h is discussed below and in Supplemental Material [28]. With $d \gtrsim 10^{-7}$ m, the PP limit of Eq. (1) is valid for $R_i \lesssim 10^{-8}$ m. Because $H \propto V_1V_2$, with V_i being the volume of particle i [see Eq. (1)], we do not give R_i explicitly and normalize the HT by V_1V_2.

Figure 2 shows the HT as a function of interparticle distance d. We note a drastic effect of the presence of the

cylinder on the far-field HT. For distances larger than a few hundred nanometers, the HT seems to be almost *independent* of distance d. This yields a strong enhancement over the vacuum HT or the case of a close-by plate, the more so, the larger d: For example, for $R = 10^{-8}$ m and $d = 10^{-1}$ m, the HT is larger than the vacuum HT by 12 orders of magnitude. In other words, the HT between the particles placed above of a wire and separated by 10 centimeters is the same as the HT between isolated particles which are just a few hundred nanometers apart. We attribute this to the system geometry, i.e., the cylinder guides the energy in the preferred direction via surface waves.

How does this effect depend on R? In Fig. 2, we note that it is especially strong for a thin cylinder, and the enhancement decreases the thicker the cylinder. For large R, the HT approaches the result of two particles close to a plate as may be expected [31]. The strong effect of a thin cylinder may be related to its ability to concentrate the near-field energy radiated by particle 1 over a smaller surface area, such that the energy loss of the surface waves traveling along the cylinder to particle 2 is minimized. Figure 3 shows the result as a function of R, for various fixed values of d, displaying the mentioned approach of the plate result for large R, and the general decrease with R. However, for very small R, the HT again decreases, so that a maximal value for R appears.

Can we characterize the observed behavior analytically? Looking at Fig. 2, one may expect that the HT decays slower than any power law. Therefore, we presumed a logarithmic dependence of $\mathrm{Tr}(\mathbb{G}\mathbb{G}^\dagger)$ for an analytical approximation of the numerical data [32], which leads to the scaling of the HT in Eq. (6). Indeed, considering a logarithmic decay with d, as well as the dependence on R and h, we found that $\mathrm{Tr}(\mathbb{G}\mathbb{G}^\dagger)$ can be well approximated by ($k = \omega/c$)

$$\mathrm{Tr}(\mathbb{G}\mathbb{G}^\dagger) \approx \frac{1}{8\pi^2 d^2}\left[1+\frac{1}{k^2d^2}+\frac{3}{k^4d^4}\right] + \frac{1}{4\pi^2k^2(R+h)^4\ln^2\left[1+\frac{\sqrt{2}\sqrt{d^2+4h^2}}{kR^2}\right]}, \tag{4}$$

where the first term is the vacuum part [12], while the second term is the cylinder contribution. Formula (4) is discussed in detail in Supplemental Material [28], where we show that it is a good approximation for almost any regimes of parameters. In case $h \ll \lambda \lesssim d$ (i.e., what we are interested in), the agreement with the numerical result is very good, and it becomes excellent when we also have $\lambda d \gg 16R^2$ or $\lambda d \ll 4R^2$. These two conditions correspond to the cylinderlike or platelike limits of $\mathrm{Tr}(\mathbb{G}\mathbb{G}^\dagger)$, respectively [28]. Substituting Eq. (4) into Eq. (1), one gets for the heat transfer

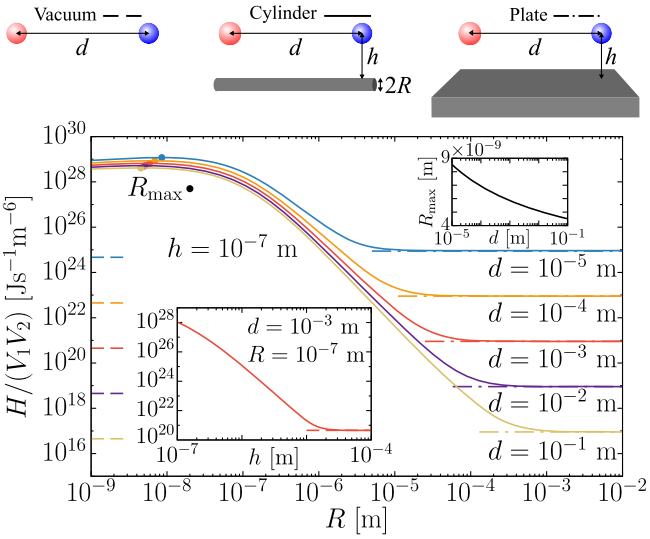

FIG. 3. Heat transfer (normalized by particles' volumes) from SiC particle 1 at temperature $T_1 = 300$ K to SiC particle 2 in the presence of a perfectly conducting cylinder as a function of its radius R. The particles are placed symmetrically above the cylinder at distance $h = 10^{-7}$ m from its surface, and the results are given for different interparticle distances d (see the sketch), using formula (6). Dashed and dashed-dotted lines give the corresponding heat transfer in vacuum and in the presence of a perfectly conducting plate (with the same h), respectively. The left inset shows H as a function of h for $d = 10^{-3}$ m and $R = 10^{-7}$ m, with the vacuum case, approached for large h, shown as a dashed line. The right inset shows $R_{\max}$ for $h = 10^{-7}$ m (the radius which maximizes the HT) as a function of d.

$$H \approx \frac{4\hbar}{\pi c^4}\int_0^\infty d\omega \frac{\omega^5}{e^{\frac{\hbar\omega}{k_B T_1}}-1}\mathrm{Im}(\alpha_1)\mathrm{Im}(\alpha_2) \times \left\{\frac{1}{d^2}\left[1+\frac{c^2}{\omega^2d^2}+\frac{3c^4}{\omega^4d^4}\right] + \frac{2c^2}{\omega^2(R+h)^4\ln^2\left[1+\frac{\sqrt{2}c\sqrt{d^2+4h^2}}{\omega R^2}\right]}\right\}. \tag{5}$$

Formula (5) can be further simplified. For SiC PPs and $T_1 = 300$ K, the HT spectrum is strongly peaked at $\omega_0 = 1.75194 \times 10^{14}$ rad s^{-1}. It is the resonance frequency of SiC PP [equivalently, the resonance frequency of α_i in Eq. (2)]. The corresponding dominant wavelength $\lambda_0 \approx 2\pi c/\omega_0 \approx 1.08 \times 10^{-5}$ m is close to λ_{T_1}. Since the cylinder is a perfect conductor, $\mathrm{Tr}(\mathbb{G}\mathbb{G}^\dagger)$ has no resonances. Therefore, we can replace ω with ω_0 in the trace and pull the trace out off the frequency integral. As a result, we finally obtain

$$H \approx \frac{4\hbar}{\pi c^4}\left\{\frac{1}{d^2}\left[1+\frac{c^2}{\omega_0^2 d^2}+\frac{3c^4}{\omega_0^4 d^4}\right] + \frac{2c^2}{\omega_0^2 (R+h)^4 \ln^2\left[1+\frac{\sqrt{2}c\sqrt{d^2+4h^2}}{\omega_0 R^2}\right]}\right\} \times \int_0^\infty d\omega \frac{\omega^5}{e^{\frac{\hbar\omega}{k_B T_1}}-1}\mathrm{Im}(\alpha_1)\mathrm{Im}(\alpha_2), \quad (6)$$

which agrees almost perfectly with Eq. (5), as shown in Supplemental Material [28], and provides a very good approximation for the exact HT, as can be seen in Fig. 2: Its inset shows that $\widetilde{H} = H(R+h)^4/(V_1 V_2 \lambda_0^2)$, plotted as a function of $\lambda_0 d/R^2$, leads to a collapse for large d of the curves for all parameters shown. Formula (6) is the main result of this Letter. It states that the HT in the presence of a cylinder decays logarithmically with d for large d, small h, and small R. More specifically, if $d \gtrsim \lambda_0$, the logarithmic behavior dominates when $h \ll \lambda_0$ and $\lambda_0 d \gg 16R^2$ [28]. Note that, for a given d and for $R \ll h$, the HT is a very strong function of h, i.e., it scales as h^{-4}. For $h \ll R$, the HT approaches an h independent value.

The logarithmic decay in Eq. (6) suggests that a cylinder is an excellent waveguide for the HT. We are not aware that any other *unconfined* geometry can outperform the one in Fig. 1 in terms of the HT efficiency for large interparticle distances. Using formula (6), the curves in Fig. 2 can be prolonged to arbitrarily large d. Imagine a thought experiment with a nanoparticle being in Minsk, while the other is in Göttingen, i.e., $d \approx 1200$ km, both placed close to an ideal nanowire ($h = R = 100$ nm). According to Eq. (6), the HT measured in such a thought experiment is the same as the HT between isolated particles separated by $d \approx 1.5$ μm. Roughly speaking, "the logarithm does not care" whether the distance is of the order of a millimeter, kilometer, or the size of the Earth.

Noting that the curves in Fig. 3 are computed using Eq. (6), they can be discussed in more detail. Interestingly, there is an optimal value of the radius, $R_{\max}$, where the HT has a maximum. This maximum slightly shifts to a smaller R with increase of d, and it lays around $R = 5 \times 10^{-9}$ m (see the right inset). For all considered d, there is a slow logarithmic growth until $R \ll h$ (encoded in the R dependence of the logarithm) followed by a fast decay ($\sim (R+h)^{-4}$) which finally bends over to the plate result. This convergence to the plate HT occurs when $4R^2 \gg \lambda_0 d$, i.e., it shifts to a larger R with increase of d [28]. Expression for the HT in the plate limit can be straightforwardly obtained from Eq. (6) using a large R expansion of the logarithm [28]. As Fig. 2, Fig. 3 reveals that a larger enhancement of the HT occurs for larger d and a thin

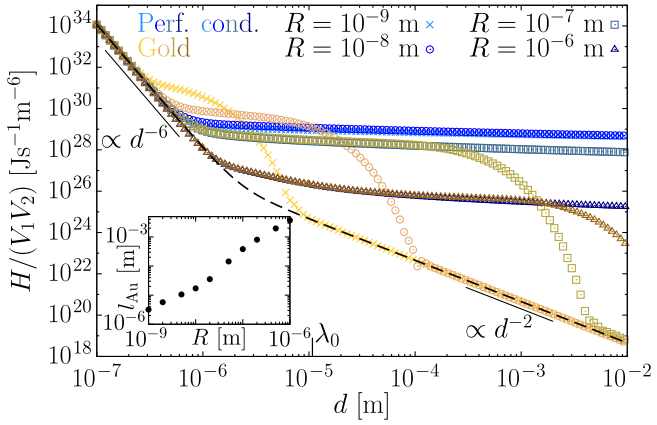

FIG. 4. Heat transfer from SiC particle 1 to SiC particle 2 as a function of d, with all parameters as in Fig. 2. Additionally to the perfectly conducting cylinder (blue shaded points) we show a gold cylinder (shades of gold). Inset shows the decay length l_{Au} (see Supplemental Material [28] for definition) for a gold cylinder, as a function of R, characterizing the transition of the HT from slow to fast decay.

cylinder. The left inset gives the HT as a function of h, which shows a strong increase with placing the particles closer to a cylinder. Note that this increase saturates once h becomes comparable to R. In Supplemental Material [28], we give the detailed R and h dependence of both numerically exact and approximated $\mathrm{Tr}(\mathbb{G}\mathbb{G}^\dagger)$ for both near- and far-field d.

As seen in Fig. 2 and Eq. (5), the HT in the presence of a cylinder follows the vacuum result until a certain distance, where it bends away and is nearly d independent. The HT with the cylinder for nearly any large d is thus comparable to the HT between isolated particles separated by a much smaller distance d_{zoom}. In other words, the cylinder allows to "zoom in" from almost any large distance to d_{zoom}. In the case of $d_{\mathrm{zoom}} \ll \lambda_0$, it reads as [found from formula (6) [28]]

$$d_{\mathrm{zoom}} \approx [\lambda_0^2 (R+h)^4]^{(1/6)}. \quad (7)$$

This zooming in is performed by bringing the particles close to the cylinder down to distance h.

What about imperfect conductors? For a real conductor, the surface waves traveling along the cylinder are damped, and the logarithmic decay is eventually cut off (see Fig. 4 and Supplemental Material [28] for details). For a gold cylinder this occurs at roughly a length of $4000R$, i.e., in the millimeter range for $R \approx 100$ nm, so that a gold microwire enhances the HT for over millimeter distances by more than 5 orders of magnitude. The amplitude of the HT generally increases for real materials, a study which we leave for future work.

Finally, it is worth mentioning that, despite the large far-field HT in the presence of a cylinder, the transferred energy is for large d small compared to the total energy

emitted by particle 1. Within the PP limit, the maximum ratio between transferred and emitted energy is around 10^{-4}, see Supplemental Material [28]. This is partly due to the observation that also the emitted energy itself increases strongly in the presence of a cylinder, as will be investigated in future work.

A cylindrical waveguide is an excellent tool to efficiently transfer thermal energy between far-separated objects. The HT efficiency with a cylinder present can be more than 10 orders of magnitude better than for isolated objects, i.e., in this aspect much better than the efficiency with other waveguide geometries [10–18]. This effect can be applied in a variety of setups, e.g., for efficient far-field cooling or heating. These findings may also drastically affect many-body effects, promising strong nonadditivity of the HT [4–6], for example, using more than one cylinder or more than two particles. A cylinder can also greatly influence the thermalization in complex setups [20,35–40] and may drastically alter the heat transfer eigenmodes [41], where the (dominant) cylinder eigenmode is expected. A highly directional energy transport with a cylinder can greatly affect heat transfer diffusion [42,43]. Using cylinders with nonreciprocal material may strongly improve rectification properties [4,5].

As for an experimental realization of the studied system, we propose using two atomic force microscope tips [44–46] placed close to a wire.

This research was funded by the Deutsche Forschungsgemeinschaft (DFG, German Research Foundation) through the Walter Benjamin fellowship (Project No. 453458207).

*asheichyk@bsu.by
†matthias.kruger@uni-goettingen.de

[1] C. Hargreaves, Phys. Lett. **30A**, 491 (1969).
[2] D. Polder and M. Van Hove, Phys. Rev. B **4**, 3303 (1971).
[3] G. Bimonte, T. Emig, M. Kardar, and M. Krüger, Annu. Rev. Condens. Matter Phys. **8**, 119 (2017).
[4] J. C. Cuevas and F. J. García-Vidal, ACS Photonics **5**, 3896 (2018).
[5] J. Song, Q. Cheng, B. Zhang, L. Lu, X. Zhou, Z. Luo, and R. Hu, Rep. Prog. Phys. **84**, 036501 (2021).
[6] S.-A. Biehs, R. Messina, P. S. Venkataram, A. W. Rodriguez, J. C. Cuevas, and P. Ben-Abdallah, Rev. Mod. Phys. **93**, 025009 (2021).
[7] V. Fernández-Hurtado, A. I. Fernández-Domínguez, J. Feist, F. J. García-Vidal, and J. C. Cuevas, Phys. Rev. B **97**, 045408 (2018).
[8] V. Fernández-Hurtado, A. I. Fernández-Domínguez, J. Feist, F. J. García-Vidal, and J. C. Cuevas, ACS Photonics **5**, 3082 (2018).
[9] D. Thompson, L. Zhu, R. Mittapally, S. Sadat, Z. Xing, P. McArdle, M. M. Qazilbash, P. Reddy, and E. Meyhofer, Nature (London) **561**, 216 (2018).
[10] K. Sääskilahti, J. Oksanen, and J. Tulkki, Phys. Rev. B **89**, 134301 (2014).
[11] R. Messina, P. Ben-Abdallah, B. Guizal, M. Antezza, and S.-A. Biehs, Phys. Rev. B **94**, 104301 (2016).
[12] K. Asheichyk, B. Müller, and M. Krüger, Phys. Rev. B **96**, 155402 (2017).
[13] J. Dong, J. Zhao, and L. Liu, Phys. Rev. B **97**, 075422 (2018).
[14] R. Messina, S.-A. Biehs, and P. Ben-Abdallah, Phys. Rev. B **97**, 165437 (2018).
[15] K. Asheichyk and M. Krüger, Phys. Rev. B **98**, 195401 (2018).
[16] Y. Zhang, M. Antezza, H.-L. Yi, and H.-P. Tan, Phys. Rev. B **100**, 085426 (2019).
[17] Y. Zhang, H.-L. Yi, H.-P. Tan, and M. Antezza, Phys. Rev. B **100**, 134305 (2019).
[18] M.-J. He, H. Qi, Y.-T. Ren, Y.-J. Zhao, and M. Antezza, Appl. Phys. Lett. **115**, 263101 (2019).
[19] A. I. Volokitin and B. N. J. Persson, Phys. Rev. B **63**, 205404 (2001).
[20] M. Krüger, G. Bimonte, T. Emig, and M. Kardar, Phys. Rev. B **86**, 115423 (2012).
[21] The particles are assumed to be nonmagnetic, i.e., their magnetic permeabilities equal unity.
[22] S. M. Rytov, Zh. Eksp. Teor. Fiz. **33**, 166 (1957) [Sov. Phys. JETP **6**, 130 (1958)].
[23] S. M. Rytov, Y. A. Kravtsov, and V. I. Tatarskii, *Principles of Statistical Radiophysics 3* (Springer, Berlin, 1989).
[24] P. Ben-Abdallah, S.-A. Biehs, and K. Joulain, Phys. Rev. Lett. **107**, 114301 (2011).
[25] R. Messina and M. Antezza, Phys. Rev. A **89**, 052104 (2014).
[26] B. Müller, R. Incardone, M. Antezza, T. Emig, and M. Krüger, Phys. Rev. B **95**, 085413 (2017).
[27] W. G. Spitzer, D. Kleinman, and D. Walsh, Phys. Rev. **113**, 127 (1959).
[28] See Supplemental Material at http://link.aps.org/supplemental/10.1103/PhysRevLett.129.170605 for the Green's function of a cylinder, dependence of $\mathrm{Tr}(\mathbb{G}\mathbb{G}^{\dagger})$ on the system parameters, details of approximation (4), comparison between Eqs. (5) and (6), details of the ratio H/H_{total}, and the heat transfer in the presence of a gold cylinder.
[29] V. A. Golyk, M. Krüger, and M. Kardar, Phys. Rev. E **85**, 046603 (2012).
[30] A. Y. Nikitin, F. J. Garcia-Vidal, and L. Martin-Moreno, IEEE J. Sel. Top. Quantum Electron. **19**, 4600611 (2013).
[31] For $d \gg \{\lambda_0, h\}$, the plate HT scales the same as the vacuum HT, i.e., $\sim d^{-2}$, but the former is two times larger [28].
[32] Logarithmic dependence on the system parameters is a known feature of a cylinder. It was observed in the heat radiation of a cylinder [29] as well as in Casimir forces involving cylinders [33,34].
[33] S. J. Rahi, T. Emig, N. Graham, R. L. Jaffe, and M. Kardar, Phys. Rev. D **80**, 085021 (2009).
[34] E. Noruzifar, T. Emig, and R. Zandi, Phys. Rev. A **84**, 042501 (2011).
[35] M. Tschikin, S.-A. Biehs, F. Rosa, and P. Ben-Abdallah, Eur. Phys. J. B **85**, 233 (2012).

[36] V. Yannopapas, J. Phys. Chem. C **117**, 14183 (2013).
[37] R. Messina, M. Tschikin, S.-A. Biehs, and P. Ben-Abdallah, Phys. Rev. B **88**, 104307 (2013).
[38] S. A. Dyakov, J. Dai, M. Yan, and M. Qiu, Phys. Rev. B **90**, 045414 (2014).
[39] M. Nikbakht, Europhys. Lett. **110**, 14004 (2015).
[40] M. Reina, R. Messina, and P. Ben-Abdallah, Phys. Rev. B **104**, L100305 (2021).
[41] S. Sanders, L. Zundel, W. J. M. Kort-Kamp, D. A. R. Dalvit, and A. Manjavacas, Phys. Rev. Lett. **126**, 193601 (2021).
[42] P. Ben-Abdallah, R. Messina, S.-A. Biehs, M. Tschikin, K. Joulain, and C. Henkel, Phys. Rev. Lett. **111**, 174301 (2013).
[43] I. Latella, S.-A. Biehs, R. Messina, A. W. Rodriguez, and P. Ben-Abdallah, Phys. Rev. B **97**, 035423 (2018).
[44] A. Narayanaswamy, S. Shen, and G. Chen, Phys. Rev. B **78**, 115303 (2008).
[45] S. Shen, A. Narayanaswamy, and G. Chen, Nano Lett. **9**, 2909 (2009).
[46] E. Rousseau, A. Siria, G. Jourdan, S. Volz, F. Comin, J. Chevrier, and J.-J. Greffet, Nat. Photonics **3**, 514 (2009).